



HHS Public Access

Author manuscript

J Drug Target. Author manuscript; available in PMC 2017 September 15.

Published in final edited form as:

J Drug Target. 2013 January ; 21(1): 44–53. doi:10.3109/1061186X.2012.725405.

Formulation and evaluation of carnosic acid nanoparticulate system for upregulation of neurotrophins in the brain upon intranasal administration

Siva Ram Kiran Vaka¹, H.N. Shivakumar², Michael A. Repka¹, and S. Narasimha Murthy¹

¹Department of Pharmaceutics, The University of Mississippi School of Pharmacy, University, MS, USA

²Department of Pharmaceutics, KLE University's College of Pharmacy, Bengaluru, Karnataka, India

Abstract

To develop formulations of carnosic acid nanoparticles and to assess their *in vivo* efficacy to enhance the expression of neurotrophins in rat model. Carnosic acid loaded chitosan nanoparticles were prepared by ionotropic gelation technique using central composite design. Response surface methodology was used to assess the effect of three factors namely chitosan concentration (0.1–1% w/v), tri-poly phosphate concentration (0.1–1% w/v) and sonication time (2–10 min) on the response variables such as particle size, zeta potential, drug encapsulation efficiency and drug release. The neurotrophins level in the rat brain upon intranasal administration of optimized batch of carnosic acid nanoparticles was determined. The experimental values for the formulation were in good agreement with those predicted by the mathematical models. A single intranasal administration of the optimized formulation of carnosic acid nanoparticles was sufficient to result in comparable levels of endogenous neurotrophins level in the brain that was almost on par with four, once a day intranasal administration of solution in rats. The results clearly demonstrated the fact that nanoparticulate drug delivery system for intranasal administration of carnosic acid would require less number of administrations to elicit the required pharmacological activity owing to its ability to localize on the olfactory mucosal region and provide controlled delivery of carnosic acid for prolonged time periods.

Keywords

Neurotrophins; carnosic acid nanoparticles; chitosan; nose to brain; Design of Experiments (DOE)

Address for Correspondence: S. Narasimha Murthy, 113 Faser Hall, Department of Pharmaceutics, The University of Mississippi, University, Mississippi 38677, USA. Tel: 662-915-5164; Fax: 662-915-1177. murthy@olemiss.edu.

Declaration of interest

The project was funded by grant # 5P20RR021929 from the National Center for Research Resources. The content is solely the responsibility of the authors and does not necessarily represent the official views of the National Center for Research Resources or the National Institutes of Health. The authors report no conflicts of interest.

Introduction

Brain targeting of drugs by intranasal route is safe, noninvasive and allows frequent administration. Therefore, it is likely that intranasal administration would be more patient compliant than the currently practiced invasive methods of treating neurodegenerative disorders such as Parkinson's disease, Alzheimer's disease, amyotrophic lateral sclerosis and Huntington's disease. These disorders are caused due to depletion of endogenous neurotrophin levels, specifically nerve growth factor (NGF) and brain derived neurotrophic factor (BDNF) which are known to play an important role in promoting the growth, differentiation and function of neurons (Martinez et al., 1985; Thorne et al., 2001; Dawbarn et al., 2003; Tapia-Arancibia et al., 2008). Restoring the levels of neurotrophins is one of the treatment approaches for the neurodegenerative disorders.

Carnosic acid (MW ~330 Da), a phenolic diterpene isolated from the leaves of *Rosemarinus officinalis* has been reported to promote the synthesis of NGF in the human glioblastoma cell lines and also enhance BDNF production in dopaminergic neuronal cell lines (Kosaka et al., 2003; Park et al., 2008; Satoh et al., 2008). The *in vivo* brain microdialysis studies carried out in Sprague Dawley rats indicated that the NGF and BDNF levels were enhanced significantly upon intranasal administration of carnosic acid solution (Vaka et al., 2011). However, nasal mucociliary clearance is one of the most important limitation that severely limits the residence time of drugs in the nasal cavity (Wang et al., 2008).

Chitosan, a polycationic derivative of chitin, is a biocompatible, biodegradable and a mucoadhesive polymer that interacts strongly with the negatively charged sialic acid residues on the mucus layer. Moreover, it has been reported to act as barrier modulating agent by improving the delivery of drugs by safe and transient permeabilization of the olfactory mucosa (Illum et al., 1994; Vaka et al., 2009). Histological studies demonstrated that chitosan has no adverse effects following frequent administration by intranasal route (Vaka et al., 2011).

Nanoparticulate drug delivery systems have been reported to improve the bioavailability of drugs upon intranasal administration as compared to drug solutions (Fernández-Urrusuno et al., 1999; Betbeder et al., 2000; Janes et al., 2001; Vila et al., 2002; Nagamoto et al., 2004). These formulations were shown to increase the residence time in the nasal cavity and also protect the drugs from the enzymatic degradation (Vila et al., 2002). Fernandez-Urrusuno et al., reported that nanoparticulate formulation of insulin was more efficient than intranasal solution in terms of reducing the plasma glucose levels (Fernández-Urrusuno et al., 1999). The better efficacy of the nanoparticulate formulation was likely due to the intensified contact of the nanoparticles with the epithelium. In another study, it was reported that cationic Biovector™ nanoparticle system formulated using polysaccharides, dipalmitoyl phosphatidyl choline and cholesterol had an extended mean residence half-life of 2.3 h in the human nasal cavity when compared to that of the residence half-life (15–30 min) of solution (Kravtsoff et al., 1998; Illum 2004). Clinical studies (Phase I) in adult human volunteers have shown that upon intranasal administration, the biovector significantly enhanced the mucosal IgA responses to two different vaccines namely virus A/Duck/Singapore (H5N3) and B/Guandong (Stephenson et al., 2006).

In the present study, the nanoparticulate system containing carnosic acid was prepared with an objective of improving the *in vivo* efficacy of carnosic acid to enhance the expression of neutrophins in the brain. The product quality attributes that would dictate the amount of carnosic acid delivered to the target site would be particle size, zeta potential, encapsulation efficiency and percentage drug release. In this context, the present work aimed to design nanoparticle formulations with most desirable features using response surface methodology (RSM). Identification of the critical process parameters that significantly influenced the product quality attributes was part of the preliminary investigations undertaken. Elucidation of the interrelationship between the independent variables and the product quality attributes followed by validation of the mathematical models were prime focus of the study that concluded with development of optimized formulations. In addition, the other objective of the proposed work was to demonstrate the *in vivo* efficacy of the nanoparticulates developed.

Materials and methods

Chemicals

Carnosic acid, chitosan, tripolyphosphate (TPP), Krebs ringer bicarbonate (KRB) buffer (premixed powder) glacial acetic acid were procured from Sigma chemicals (St. Louis, MO, USA). Hydroxy propyl-beta-cyclodextrin (HP- β -CD) was procured from Roquette Pharma (Keokuk, IA, USA). NGF and BDNF E_{\max} ® Immunoassay systems were purchased from Promega Corporation (Madison, WI, USA). All other reagents and solvents used were of analytical grade.

Analytical method

The amount of carnosic acid in the samples collected from various studies was quantified using high performance liquid chromatography (HPLC) system (Waters, 1525) with an autosampler (Waters, 717 plus), consisting of a Phenomenex C18 (2) 100 R analytical column (4.6 mm \times 150 mm, Luna, 5.0 mm) and a dual λ absorbance detector (Waters, 2487). Mobile phase consisted of acetonitrile and 0.1% phosphoric acid solution (55:45, v/v) (Yan et al., 2009). Elution was performed isocratically at 25°C at a flow rate of 1.5 mL/min. Injection volume was 100 μ L and the column effluent was monitored at 210 nm. The range for the calibration curve was 5–1000 ng/mL ($R^2 = 0.99$).

Formulation of nanoparticles

Design of Experiment (DOE)—A set of preliminary studies undertaken indicated that TPP concentration (X_1) and chitosan concentration (X_2) as well as the sonication time (X_3) critically affected the quality attributes of the nanoparticles in a nonlinear fashion. Considering this, a 20-run, 3_3 Face centered design consisting of 3 factors at 3 levels was set up using Design-Expert® 8.0.2 version software to produce the carnosic acid loaded chitosan nanoparticles. The design composed of eight factorial points, six axial points and six center points. The effect of the critical independent variables/factors on the product quality attributes/responses like average particle size (Y_1), zeta potential (Y_2), percent drug encapsulation efficiency (Y_3) and percent drug release at 12th h (Y_4) were systematically

investigated. The factors and the corresponding levels as per the design have been represented in Table 1.

Carnosic acid loaded chitosan nanoparticles were prepared by ionic interaction with TPP as per the experimental design. Different concentrations of chitosan solutions as per the table were prepared by dissolving required quantity of chitosan in KRB buffer containing 1% glacial acetic acid. Simultaneously, carnosic acid was dissolved in the second portion of the buffer that contained 20% HP- β -CD. The two solutions were then mixed together with required concentration of TPP solution as per the design. The resulting solution was ultrasonicated using a very high intensity microprobe with a diameter of 3.2 mm and a 100 W high intensity processor (Microson XL-2000, VWR International, West Chester, PA, USA). The probe was immersed into the solution and ultrasonication was carried out for the stipulated time period as per the design to produce carnosic acid loaded chitosan nanoparticles. The independent variables employed to produce 20 batches of nanoparticles as per the experimental design is portrayed in Table 2. The nanoparticles produced were characterized immediately.

Characterization of nanoparticles

The different model formulations were diluted to two-folds and the particle size and zeta potential were determined using Zetasizer Nano-ZS (Malvern Instruments Inc., Westborough, MA, USA). The particle size was measured by photon correlation spectroscopy (PCS or dynamic light scattering, DLS), which is a powerful tool for estimating the particle size of fine particles ranging from a few nanometers to micrometers (Komatsu et al., 1995). The zeta potential was determined based on electrophoretic light scattering technique.

Determination of encapsulation efficiency

The encapsulation efficiency of different formulations was determined by separating the nanoparticles from the aqueous suspension containing non-entrapped carnosic acid. The separation was accomplished by taking 200 μ L of formulation in 0.5 mL centrifugal filter units and centrifuging at 5000 rpm for 7 min. The solution collected in the tube after centrifugation was suitably diluted and analyzed by HPLC to determine the amount of free carnosic acid. The percentage encapsulation efficiency (% EE) was calculated according to the equation below:

$$\%EE = \frac{\text{Total amount of carnosic acid} - \text{Free amount of carnosic acid}}{\text{Total amount of carnosic acid}} \times 100$$

***In vitro* release study**—Carnosic acid release from the model formulations was determined by taking 1 mL of the nanoparticle formulation in a dialysis bag clamped at both ends. The dialysis bag was then suspended in a beaker containing 100 mL of 20 % HP- β -CD solution that was slowly stirred using a magnetic bead at room temperature. Samples (10 mL) were withdrawn at regular intervals of time up to 12 h and replaced with same volume of 20% HP- β -CD solution to maintain sink conditions. The collected samples were diluted accordingly and quantified by HPLC.

Regression analysis

The response parameters were statistically analyzed by applying one-way ANOVA at 0.05 level. The individual parameters were evaluated using the F test and Quadratic models as shown in equation were generated for each response using multiple linear regression analysis

$$Y = \beta_0 + \beta_1 X_1 + \beta_2 X_2 + \beta_3 X_3 + \beta_4 X_1^2 + \beta_5 X_2^2 + \beta_6 X_3^2 + \beta_7 X_1 X_2 + \beta_8 X_1 X_3 + \beta_9 X_2 X_3$$

Where Y is the level of the measured response, β_0 is the intercept, β_1 – β_9 are the regression coefficients, X_1 , X_2 , X_3 stand for the main effects, $X_1 X_2$, $X_2 X_3$, $X_1 X_3$ represent the two-way interaction terms while $X_1 X_2 X_3$ stands for three-way interaction. The quadratic terms that were used to simulate the curvature of the design space are represented by X_1^2 , X_2^2 and X_3^2 . A backward elimination process was performed to reduce the mathematical models in order to include only the significant terms and preclude the insignificant terms. The mathematical models generated by regression analysis were used to construct the 3-dimensional (3-D) graphs where the response parameter Y was represented by a curvature surface as a function of X. The effects of the critical factors on the response parameters were visualized from the contour plots.

Optimization

An attempt was made to validate the mathematical models generated and at the same time develop a set of optimized formulations with the most desirable product quality attributes. The constraints set to locate the optimal settings of the new formulations with intent to enhance the amount of carnosic acid delivered to the brain are outlined in Table 1. The three new formulations developed were evaluated for the product quality attributes, and the experimental values obtained were compared with those predicted by the mathematical models. The optimized formulation that displayed the least prediction error was considered for further *in vivo* studies in rat model.

In vitro mucoadhesion studies

These studies were carried out using bovine olfactory mucosa used as a substrate. A known amount of nanoparticles (100 mg) of the optimized batch was sprinkled on to the mucosa which was mounted on a glass slide. Then the glass slide was placed in desiccator for about 15 min so as to allow the polymer to interact with the membrane. After 15 min, the glass slide was taken out from the desiccator and was placed at an angle of 45°. The KRB buffer was run over the mucosa at the rate of 100 μ L/min and the washings were collected and freeze dried. The weight of nanoparticles washed out was determined at predetermined time points for 6 h and the percent mucoadhesion was calculated as follows (Nanjwade et al., 2011).

$$\% \text{mucoadhesion} = \frac{(W_i - W_f) \times 100}{W_i}$$

Where, W_i is the weight of the nanoparticles applied to the mucosa and W_f represents the weight of the nanoparticles washed out.

***In vivo* studies**

In vivo evaluation of the optimized batch of nanoparticles were carried out in male, Sprague–dawley rats (250–300 g, Harlan Company, Indianapolis, IN) under anesthesia [ketamine (80 mg/kg) + xylazine (10 mg/kg); i.p injection]. The experimental procedures were approved by the Institutional Animal Care and Use Committee (IACUC) at the University of Mississippi (Protocol # 10–017). The rats were divided into three groups based on the type and/or duration of administration of the formulation, (i) solution (administered only once), (ii) solution (administered daily once for 4 days) and (iii) nanoparticulate formulation (administered only once). Each of these group of rats is further divided into three subgroups ($n = 3$) each.

The rats of subgroup 1 were administered with 0.25% w/v chitosan (vehicle control), while subgroup 2 rats were administered with chitosan solution containing nanoparticles of the optimized batch (at a dose of 4 mg carnosic acid/kg) via intranasal route and subgroup 3 rats were administered with chitosan solution containing nanoparticles at the same dose by subcutaneous injection. The formulations were administered intranasally (subgroups 1 & 2) by placing the anesthetized rats on their back and by inserting the soft polymer capillary connected to a microsyringe into the posterior segment of the nose. After 4 days the rats were anesthetized and the neurotrophins in the brain were sampled by microdialysis. Briefly, the rats were secured on the stereotaxic frame (Harvard Instruments, Holliston, MA) and the probe (CMA 12) was implanted into the hippocampal region (anterior-posterior = 5.6 mm, medio-lateral = 5 mm, dorso-ventral = 7 mm, from bregma) (Vaka et al., 2009). Initially, the microdialysis probes were equilibrated by perfusing KRB buffer at the rate of 2 μ L/min using a microinjection pump for a period of 1 h. The microdialysis samples were collected and assayed for NGF and BDNF by enzyme-linked immunosorbent assay. The sensitivity of the assay was \sim 7.8 pg/mL.

Results and discussion

Central composite design (CCD) is a well suited RSM employed for fitting a quadratic surface. This design is one of the commonly used RSM designs for process optimization. CCD is used to establish the design space and optimize the process parameters with lesser number of runs compared to other RSM designs. CCD was opted in the present context since the preliminary studies undertaken revealed that the critical factors affected the product quality attributes of the nanoparticles in a nonlinear fashion.

Face Centered Design (FCD) is a type of CCD which provides relatively high quality predictions over the entire design space. In addition, the design is said to have good design properties like little co-linearity and is insensitive to outliers and missing data.

Chitosan nanoparticles are generally formulated by chemical cross-linking with different kinds of polyanions (glycyrrhetic acid, polyaspartic acid, etc.) and other oppositely charged molecules yielding controlled drug release formulations with less toxicity (Zheng et al.,

2006; Zheng et al., 2007). However, the most extensively used polyanion to cross-link chitosan is triphosphosphate. Chitosan – TPP nanoparticles were formed by means of electrostatic interaction between the positively charged amino groups of chitosan and negatively charged phosphate and hydroxide groups of TPP, which compete with each other to interact with amino groups of chitosan (Bhumkar et al., 2006). The nanoparticles formed by this type of interaction were reported to have strong adhesion and immediate immobilization on to negatively charged mucosal surfaces (Vila et al., 2004).

From the preliminary studies it was found that the inherent aqueous solubility of carnosic acid is poor. Hence, HP- β -CD was used in the present studies to retain the relatively hydrophobic carnosic acid in the aqueous solution prior to encapsulation with the chitosan. Our earlier studies have indicated that solubility of carnosic acid was enhanced by ~900-fold at 20% HP- β -CD over its inherent solubility in KRB buffer (Vaka et al., 2011). During the preparation, chitosan and TPP concentrations in the buffer as well as the sonication time were varied as per the experimental plan, while the non-DOE variables were held constant.

Partice size and zeta potential of nanoparticles

The particle size is a key parameter that is assumed to affect the drug release kinetics and eventually dictate the amount delivered to the target site. The size of the nanoparticles of different model formulation is captured in Table 3. The different model formulations of nanoparticles were found to range in size from 182.34 ± 15.40 to 831.25 ± 20.94 nm. Chitosan concentration was the only factor that was found to have a profound effect on the nanoparticle size while the TPP concentrations and the sonication time failed to have a big impact on the particle size. Solutions containing higher concentrations of chitosan due to the higher visocities produced relatively bigger nanoparticles that ranged in size between 374.67 ± 10.86 and 831.25 ± 20.94 nm. On the contrary, lower concentrations of chitosan formed finer nanoparticles that varied in the size between 182.34 ± 15.40 and 345.27 ± 37.30 nm. The variation in particle size could be attributed to the change in viscosity of the polymer solutions with the change in chitosan concentration.

Zeta potential plays an important role in the interactions with mucin glycoproteins present in the olfactory mucosa. Zeta potential could also be useful indicator of the physical stability of the nanoparticles. The zeta potential of the different model formulations was found to vary from 16.4 ± 2.3 to 38.6 ± 2.8 mV (Table 3). TPP concentration was the only factor that demonstrated a substantial impact on the zeta potential. The zeta potential assumed relatively higher values (24.00 ± 0.82 to 38.6 ± 2.8 mV) at lower concentrations of TPP, while the potential dropped (16.4 ± 2.3 to 23.6 ± 1.09 mV) at higher TPP concentrations. The changes in the zeta potential can be ascribed to the changes in the net charge carried by the particles that resulted from the interaction of the polyanionic TPP and polycationic chitosan. The higher the absolute value of zeta potential, greater would be the charges on the dispersed particles and lesser are the chances of aggregation. Therefore, a higher zeta potential is recommended in the present case to retain the particles as individual entities and to enhance the stability of the nanoparticle formulation. Moreover, the positive charge on the particles could also favor their retention on the olfactory mucosa which bears a net negative charge like most other epithelial layers.

Encapsulation efficiency and *in vitro* drug release

The percentage encapsulation efficiency indicates the amount of carnosic acid encapsulated within the nanoparticles. The incorporation of therapeutic agents into nanoparticles would be governed by the method of preparation, drug and polymer concentrations, drug physicochemical characteristics and nanoparticles size. The physicochemical property of carnosic acid was positively modified in the present study by using a complexing agent like HP- β -CD so as to facilitate the encapsulation of the relatively hydrophobic active in the hydrophilic chitosan. The encapsulation efficiency of different model formulations was found to range from 40.98 ± 4.72 to $86.94 \pm 2.03\%$ as shown in Table 3. The concentration of chitosan was found to have a considerable influence on the encapsulation efficiency of the nanoparticles. The encapsulation efficiencies were found to be poor (40.98 ± 4.72 to $57.32 \pm 1.51\%$) at high chitosan concentrations while it improved (64.57 ± 1.03 to $86.94 \pm 2.03\%$) as the chitosan concentrations were decreased. Low chitosan concentrations owing to the low viscosities, tend to reduce the liquid phase resistance during dispersion which in turn would have promoted the encapsulation of the drug into the nanoparticles whereas, the highly viscous nature of chitosan solution at higher polymer concentrations is more likely to hinder the drug encapsulation.

The release of carnosic acid from chitosan nanoparticles was performed in 20% HP- β -CD aqueous solution so as to maintain a sink condition. The percentage drug released at the end of 12 h for different model formulations was found to vary from 17.01 ± 2.96 to $52.52 \pm 2.08\%$ as indicated in Figure 1.

The amount of carnosic acid released was found to depend on the chitosan concentrations used to produce the nanoparticles (Table 3). The percentage drug released decreased (17.01 ± 2.96 to $23.58 \pm 1.55\%$) with increase in the chitosan concentrations, while increased (29.33 ± 1.57 to $52.52 \pm 2.08\%$) at low chitosan concentrations. The differences in the drug release can be directly related to the change in the particle size which in turn was dictated by chitosan concentrations. Higher release of carnosic acid was observed in case of relatively smaller particles which were formed at lower chitosan concentrations whereas, a slower release was seen with larger nanoparticles produced at high chitosan concentrations.

Regression analysis

The results of the ANOVA and the mathematical models generated are outlined in Table 4. The Fischer F test with a low probability value ($P_{\text{model}} > F$ less than 0.0001) demonstrated a very high significance of the predictor model generated for the particle size. The value of the adjusted determination coefficient (adjusted $R^2 = 0.72$) was in agreement with that of the determination coefficient ($R^2 = 0.75$) indicating the goodness-of-fit of the mathematical model. It was also noticeable that the adjusted R^2 approached a value close to one as the model was reduced by excluding the insignificant terms. A high value of the correlation coefficient ($R = 0.87$) signified an excellent correlation between the independent factors.

The mathematical model suggested that the chitosan concentration ($P > F$ less than 0.0001) as well as the TPP concentration ($P > F = 0.029$) significantly influenced the particle size of the nanoparticles though the positive effect of the former was dominant. The predominant

influence of chitosan on the particle size of the nanoparticles was clearly evident from the model generated (Table 4) and the 3-D plots (Figure 2). The corresponding contour plots were linear suggesting that the target particle size of 250 nm can be achieved using low concentrations of chitosan. Though TPP concentrations negatively affected the particle size, the effect seemed to be too meager to counteract the positive influence of the chitosan concentration.

The F test indicated that the mathematical model generated for the zeta potential was highly significant ($P_{\text{model}} > F$ less than 0.0001). The value of adjusted determination coefficient (adjusted $R^2 = 0.64$) was found to be in agreement with the value of determination coefficient ($R^2 = 0.68$) indicating the goodness-of-fit of the model generated. A high value of the correlation coefficient ($R = 0.82$) indicated an excellent correlation between the independent factors.

The predictor model generated for zeta potential suggested that TPP concentration emerged as the factor with highest statistical significance ($P > F$ less than 0.0001). The negative influence of the TPP concentrations on the zeta potential of the nanoparticles was evident from the predictor model (Table 4) and the 3-D plots (Figure 3). The corresponding contour plots demonstrated a linear trend suggesting that zeta potential declined with increase in the TPP concentrations. The plots depicted that the target zeta potential of 30 mV could be attained at low to intermediate concentrations of TPP coupled with intermediate to high concentrations of chitosan. Although, chitosan concentrations significantly affected the zeta potential ($P > F = 0.01$), the influence looked too feeble compared to that of TPP.

The F test with a low probability value ($P_{\text{model}} > F$ less than 0.0001) indicated that all the three independent factors significantly influenced the encapsulation efficiency. The value of the adjusted determination coefficient (adjusted $R^2 = 0.89$) was in agreement with the value of the determination coefficient ($R^2 = 0.93$) indicating the goodness-of-fit of the mathematical model. The value of correlation coefficient ($R = 0.96$) approached unity as the model was refined by eliminating the insignificant terms. A high value of the correlation coefficient signified an excellent correlation between all the three independent factors.

The quadratic model generated suggested that all the three variables namely chitosan concentration ($P > F$ less than 0.0001), TPP concentration ($P > F$ less than 0.0009) and sonication time ($P > F$ less than 0.0307) significantly influenced the encapsulation efficiency. It was noted that chitosan concentration was the most influential followed by TPP concentration and finally the sonication time which was the least. In addition to the main effects the quadratic terms also affected the encapsulation efficiency.

The negative influence of chitosan on the encapsulation efficiency of the nanoparticles has been captured in the 3-D plot depicted in Figure 4. The corresponding contour plots demonstrated a curvilinear trend suggesting that the encapsulation efficiency could be maximized at low concentrations of chitosan. However, a direct relationship between the three independent variables and encapsulation efficiency could not be clearly elucidated owing to the involvement of the quadratic terms in the model.

The F test indicated that the mathematical model generated for drug release at 12 h was highly significant ($P_{\text{model}} > F$ less than 0.0001). The value of the adjusted determination coefficient (adjusted $R^2 = 0.64$) was found to be in reasonable agreement with the value of determination coefficient ($R^2 = 0.68$) indicating the goodness-of-fit of the model. A high value of the correlation coefficient ($R = 0.82$) indicated an excellent correlation between the independent variables.

The regression model generated for the drug release at 12 h suggested that the chitosan concentration ($P > F$ less than 0.0001) and the TPP concentration ($P > F$ less = 0.0351) had a significant influence on the response though the effect of the latter was marginal. The negative influence of chitosan in particular on the drug release was evident from the 3-D plots (Figure 5) and the mathematical model (Table 4). The corresponding contour plots were linear and suggested that drug release was more controlled as the chitosan concentrations increased. The plots depicted that the drug release of 50% at 12 h could be attained at low settings of chitosan and TPP concentrations.

In summary, chitosan concentration was the most influential factor that had affected the particle size, encapsulation efficiency and drug release of the nanoparticles. On the other hand, TPP concentrations had a good impact on the zeta potential whereas, the sonication time had a trivial influence on the encapsulation efficiency. An insignificant lack of fit (LOF) implied a good fitment of the all mathematical models generated indicating that the models can be used as response predictors. Model reduction by eliminating the insignificant terms is likely to improve the prognostic capability of the mathematical models generated.

Optimization

The mathematical models generated were validated by preparing three new formulations which differed totally in composition and processing time from the model formulations. A numerical optimization technique employing desirability approach was used to locate the optimum settings of the new formulations. Various feasibility and grid searches were executed to establish the composition of these optimized formulations. The three new formulations developed were evaluated and the experimental values of the responses were compared with those predicted by the mathematical models.

The comparison of the two sets of values along with the prediction error involved is shown in Table 5. The prediction error for the response parameters of formulation 23 was found to be ranging from -4.19 to 14.48, which was much lesser than the prediction errors associated with formulations 21 and 22. The low values of the prediction error proved the validity of the mathematical models and clearly demonstrated the prognostic potential of the models generated by MLRA and ANOVA. Considering the low prediction error, formulation 23 was taken further for *in vitro* mucoadhesion and *in vivo* studies.

The *in vitro* mucoadhesion studies carried using bovine olfactory mucosa as a substrate indicated that the nanoparticles developed by ionotropic gelation method were found to exhibit good mucoadhesion. However, a marginal decline in the percent mucoadhesion was noted (from $86 \pm 2.23\%$ to $73 \pm 3.2\%$) over a period of 6 h justifying the selection of the polymer and the cross linking agent (Figure 6). The result of the studies also authenticated

the optimal settings of the materials used to produce the new formulations. The promising results with the formulation 23 emphasized the need for further *in vivo* studies.

***In vivo* studies**

The recovery studies of the microdialysis probes was determined *in vitro* and was found to be $4.2 \pm 0.3\%$ and $2.98 \pm 0.2\%$ in studies carried out using NGF and BDNF, respectively. In case of rats belonging to group B, upon intranasal administration of 0.25% w/v chitosan solution (vehicle control group) to subgroup 1, the endogenous NGF and BDNF levels were found to be 124.01 ± 28.06 ng/L and 206.91 ± 50.94 ng/L, respectively. Whereas, upon intranasal administration of 4 mg/kg carnosic acid solution with chitosan (0.25% w/v) to subgroup 2 rats the NGF levels were enhanced by ~3.2-fold and the BDNF levels by ~2.7-fold as compared to control subgroup. However, when carnosic acid solution (4 mg/kg) was administered via subcutaneous route (subgroup 3) there was ~50% increase in the BDNF and NGF levels in the brain compared to control subgroup indicating that parenteral administration would deliver effective levels of carnosic acid into brain. However, frequent administration and invasiveness limits the parenteral route. Interestingly, when the formulations were administered to all the 3 subgroups of rats in the form of nanoparticles (Group C) only once in contrary to that of solution which was administered daily once for a period of 4 days (Group B), there was no statistically significant difference in the endogenous NGF and BDNF levels (Figure 7). These results clearly indicate the potential of the nanoparticulate system in maintaining therapeutic levels for an extended period of time even upon single administration. Moreover, when the formulations were administered in the form of solution only once to the rats belonging to group A, the NGF and BDNF levels in all the 3 subgroups of rats even after 4 days were not statistically significant from the vehicle control subgroup.

Conclusions

Carnosic acid nanoparticles were developed by ionotropic gelation technique using response surface methodology and were assessed *in vivo*. These studies clearly indicate that the carnosic acid loaded chitosan nanoparticles might represent a promising platform for upregulation of neurotrophins in the brain upon intranasal administration. The proposed system is also likely to reduce the frequency of administration by maintaining prolonged therapeutic levels due to higher retention time at the site of delivery.

References

- Betbeder D, Spérandio S, Latapie JP, de Nadai J, Etienne A, Zajac JM, Francés B. Biovector nanoparticles improve antinociceptive efficacy of nasal morphine. *Pharm Res.* 2000; 17:743–748. [PubMed: 10955851]
- Bhumkar DR, Pokharkar VB. Studies on effect of pH on cross-linking of chitosan with sodium tripolyphosphate: a technical note. *AAPS PharmSciTech.* 2006; 7:E50. [PubMed: 16796367]
- Dawbarn D, Allen SJ. Neurotrophins and neurodegeneration. *Neuropathol Appl Neurobiol.* 2003; 29:211–230. [PubMed: 12787319]
- Fernández-Urrusuno R, Calvo P, Remuñán-López C, Vila-Jato JL, Alonso MJ. Enhancement of nasal absorption of insulin using chitosan nanoparticles. *Pharm Res.* 1999; 16:1576–1581. [PubMed: 10554100]

- Illum L. Is nose-to-brain transport of drugs in man a reality? *J Pharm Pharmacol.* 2004; 56:3–17. [PubMed: 14979996]
- Illum L, Farraj NF, Davis SS. Chitosan as a novel nasal delivery system for peptide drugs. *Pharm Res.* 1994; 11:1186–1189. [PubMed: 7971722]
- Janes KA, Calvo P, Alonso MJ. Polysaccharide colloidal particles as delivery systems for macromolecules. *Adv Drug Deliv Rev.* 2001; 47:83–97. [PubMed: 11251247]
- Komatsu H, Kitajima A, Okada S. Pharmaceutical characterization of commercially available intravenous fat emulsions: estimation of average particle size, size distribution and surface potential using photon correlation spectroscopy. *Chem Pharm Bull.* 1995; 43:1412–1415. [PubMed: 7553988]
- Kosaka K, Yokoi T. Carnosic acid, a component of rosemary (*Rosmarinus officinalis* L.), promotes synthesis of nerve growth factor in T98G human glioblastoma cells. *Biol Pharm Bull.* 2003; 26:1620–1622. [PubMed: 14600414]
- Kravtsoff R, Fisher A, De Miguel I, Perkins A, Major M, Betbeder D, Etienne A. Nasal residence time evaluation of cationic Biovector™ in human volunteers. *Proc Int Symp Control Rel Bioact Mater.* 1998; 25:818–819.
- Martínez HJ, Dreyfus CF, Jonakait GM, Black IB. Nerve growth factor promotes cholinergic development in brain striatal cultures. *Proc Natl Acad Sci USA.* 1985; 82:7777–7781. [PubMed: 3865196]
- Nagamoto T, Hattori Y, Takayama K, Maitani Y. Novel chitosan particles and chitosan-coated emulsions inducing immune response via intranasal vaccine delivery. *Pharm Res.* 2004; 21:671–674. [PubMed: 15139524]
- Nanjwade B, Parikh K, Deshmukh R, Nanjwade V, Gaikwad K. Development and evaluation of intranasal mucoadhesive microspheres of neostigmine bromide. *Pharm Anal Acta.* 2011; 2:2.
- Park JA, Kim S, Lee SY, Kim CS, Kim do K, Kim SJ, Chun HS. Beneficial effects of carnosic acid on dieldrin-induced dopaminergic neuronal cell death. *Neuroreport.* 2008; 19:1301–1304. [PubMed: 18695511]
- Satoh T, Kosaka K, Itoh K, Kobayashi A, Yamamoto M, Shimojo Y, Kitajima C, Cui J, Kamins J, Okamoto S, Izumi M, Shirasawa T, Lipton SA. Carnosic acid, a catechol-type electrophilic compound, protects neurons both *in vitro* and *in vivo* through activation of the Keap1/Nrf2 pathway via S-alkylation of targeted cysteines on Keap1. *J Neurochem.* 2008; 104:1116–1131. [PubMed: 17995931]
- Stephenson I, Zambon MC, Rudin A, Colegate A, Podda A, Bugarini R, Del Giudice G, Minutello A, Bonnington S, Holmgren J, Mills KH, Nicholson KG. Phase I evaluation of intranasal trivalent inactivated influenza vaccine with nontoxigenic *Escherichia coli* enterotoxin and novel biovector as mucosal adjuvants, using adult volunteers. *J Virol.* 2006; 80:4962–4970. [PubMed: 16641287]
- Tapia-Arancibia L, Aliaga E, Silhol M, Arancibia S. New insights into brain BDNF function in normal aging and Alzheimer disease. *Brain Res Rev.* 2008; 59:201–220. [PubMed: 18708092]
- Thorne RG, Frey WH 2nd. Delivery of neurotrophic factors to the central nervous system: pharmacokinetic considerations. *Clin Pharmacokinet.* 2001; 40:907–946. [PubMed: 11735609]
- Vaka SRK, Murthy SN, Repka MA, Nagy T. Upregulation of endogenous neurotrophin levels in the brain by intranasal administration of carnosic acid. *J Pharm Sci.* 2011; 100:3139–3145. [PubMed: 21360710]
- Vaka SRK, Sammeta SM, Day LB, Murthy SN. Delivery of nerve growth factor to brain via intranasal administration and enhancement of brain uptake. *J Pharm Sci.* 2009; 98:3640–3646. [PubMed: 19156912]
- Vila A, Sánchez A, Janes K, Behrens I, Kissel T, Vila Jato JL, Alonso MJ. Low molecular weight chitosan nanoparticles as new carriers for nasal vaccine delivery in mice. *Eur J Pharm Biopharm.* 2004; 57:123–131. [PubMed: 14729088]
- Vila A, Sánchez A, Tobío M, Calvo P, Alonso MJ. Design of biodegradable particles for protein delivery. *J Control Release.* 2002; 78:15–24. [PubMed: 11772445]
- Wang X, Chi N, Tang X. Preparation of estradiol chitosan nanoparticles for improving nasal absorption and brain targeting. *Eur J Pharm Biopharm.* 2008; 70:735–740. [PubMed: 18684400]

- Yan H, Wang L, Li X, Yu C, Zhang K, Jiang Y, Wu L, Lu W, Tu P. High-performance liquid chromatography method for determination of carnosic acid in rat plasma and its application to pharmacokinetic study. *Biomed Chromatogr.* 2009; 23:776–781. [PubMed: 19309757]
- Zheng Y, Wu Y, Yang W, Wang C, Fu S, Shen X. Preparation, characterization, and drug release *in vitro* of chitosan-glycyrrhetic acid nanoparticles. *J Pharm Sci.* 2006; 95:181–191. [PubMed: 16315245]
- Zheng Y, Yang W, Wang C, Hu J, Fu S, Dong L, Wu L, Shen X. Nanoparticles based on the complex of chitosan and polyaspartic acid sodium salt: preparation, characterization and the use for 5-fluorouracil delivery. *Eur J Pharm Biopharm.* 2007; 67:621–631. [PubMed: 17533123]

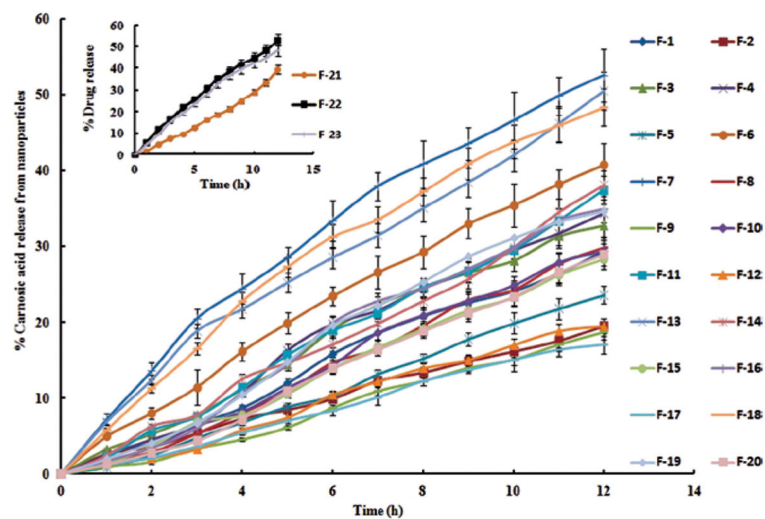


Figure 1. *In vitro* drug release from the model and optimized (insert graph) formulations of nanoparticles. Data expressed as mean \pm SD ($n = 3$).

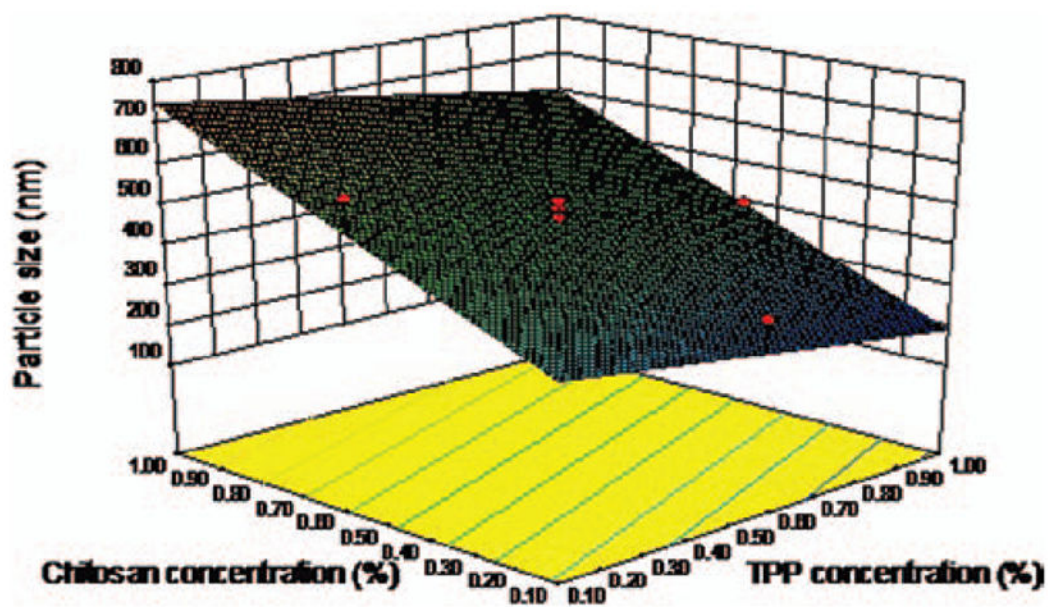


Figure 2.
Plot showing the influence of chitosan and TPP concentrations on the particle size of carnosic acid loaded chitosan nanoparticles.

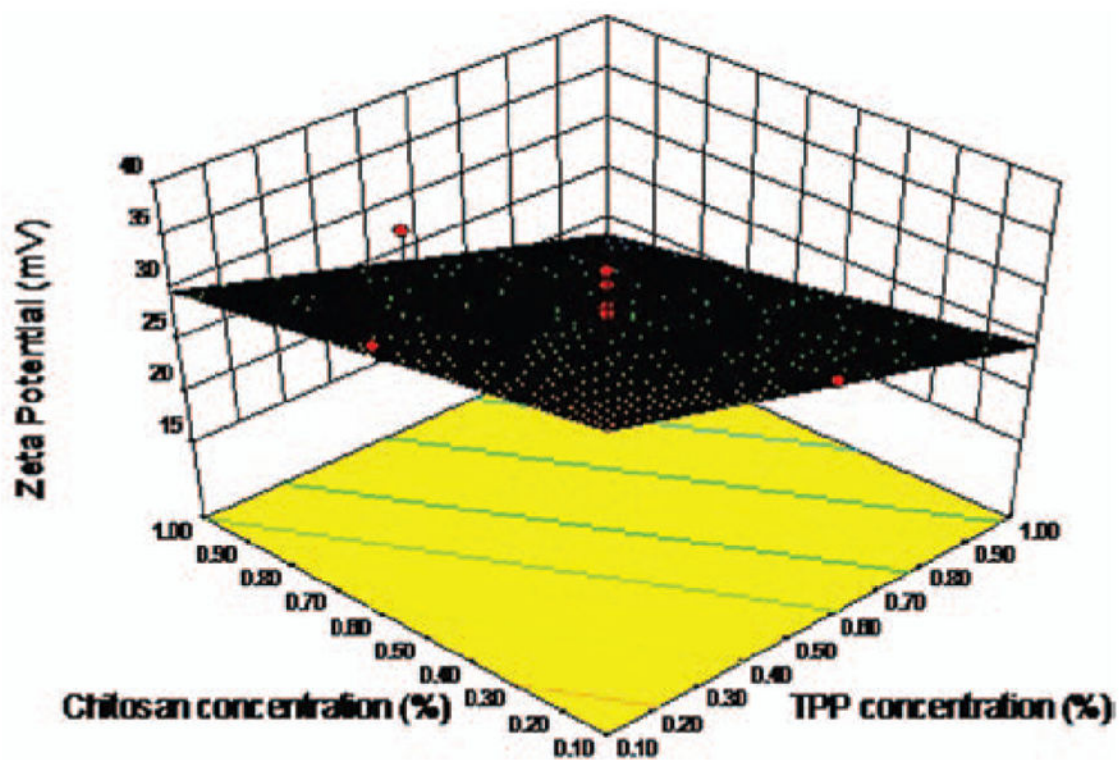


Figure 3.
Plot showing the influence of TPP and chitosan concentrations on the zeta potential carried by carnosic acid loaded chitosan nanoparticles.

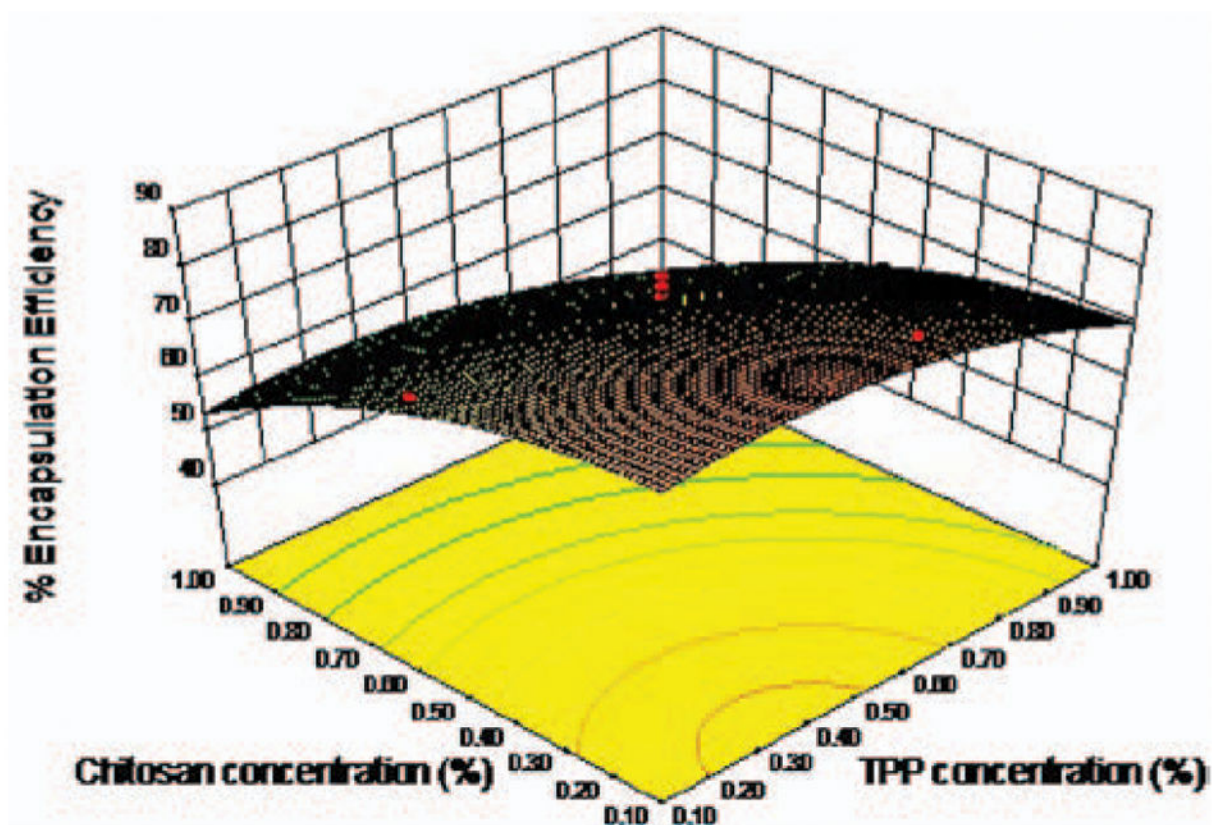


Figure 4. Plot showing the influence of chitosan and TPP concentrations on the percent encapsulation efficiency of carnosic acid loaded chitosan nanoparticles.

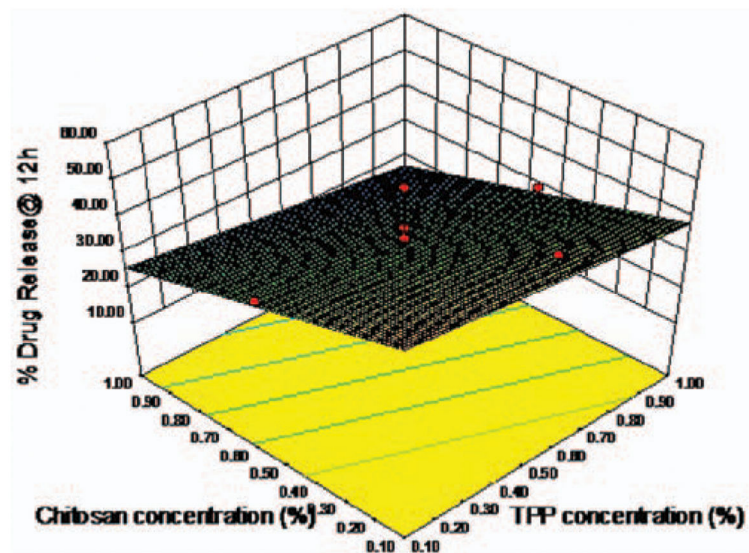


Figure 5. Plot showing the influence of chitosan and TPP concentrations on the percent drug release at 12 h from carnosic acid loaded chitosan nanoparticles.

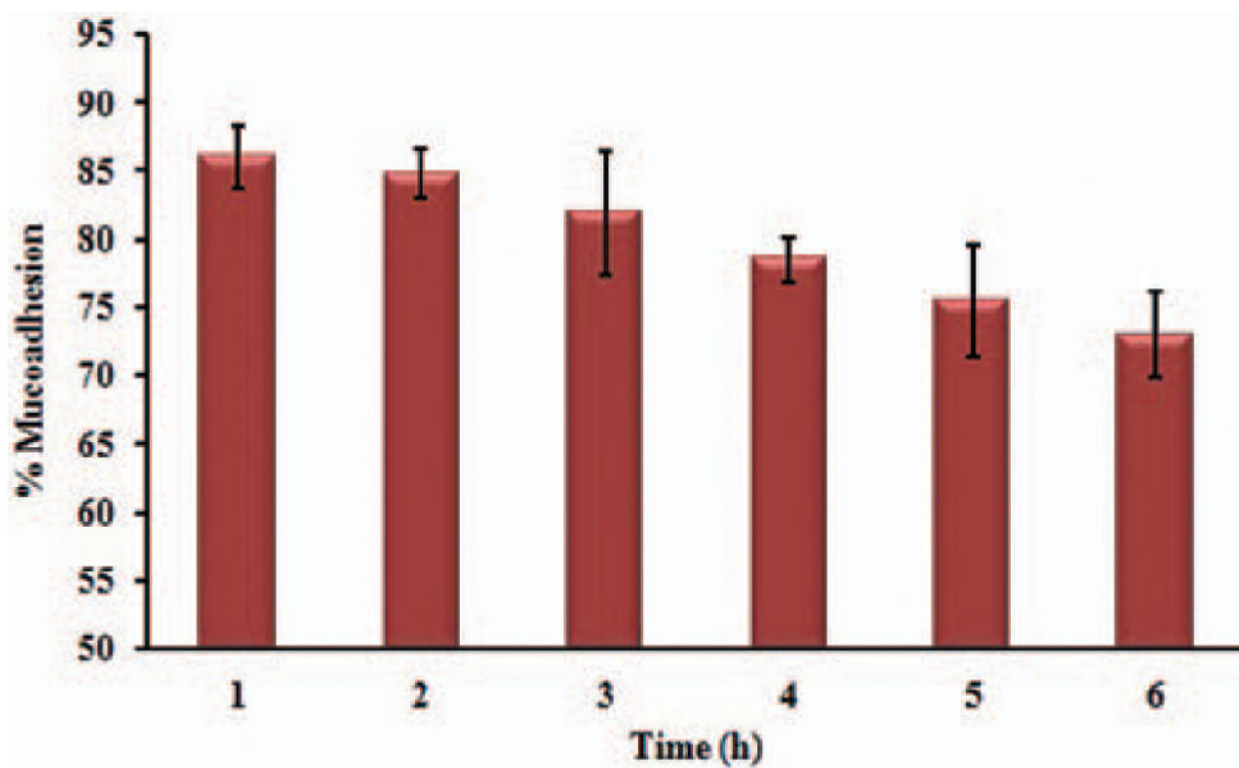


Figure 6.
In vitro mucoadhesion studies of nanoparticles (formulation 23) using bovine olfactory mucosa as substrate. Data expressed as mean \pm SD ($n = 3$).

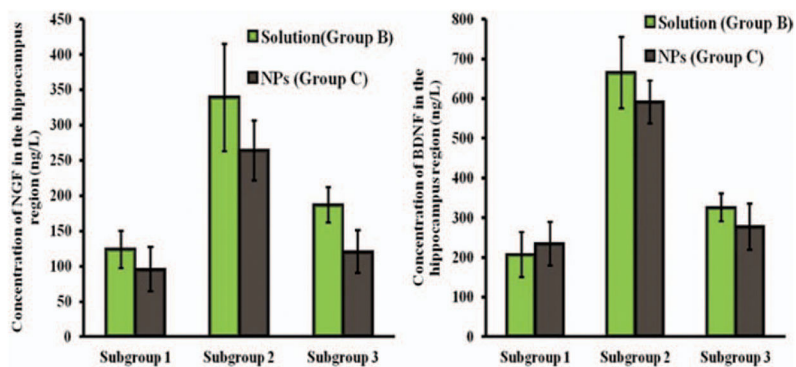


Figure 7. Concentration of (a) nerve growth factor (NGF) and (b) brain derived neurotrophic factor (BDNF) in the rat hippocampus upon intranasal/subcutaneous administration of the formulations. The data points represent average values of three animals with standard error of mean as error bars.

Table 1

Factors and the corresponding levels for the preparation of carnosic acid loaded chitosan nanoparticles by ionic interaction as per 33 Face centered design.

Input variables/Independent factors	Low level	High level
X ₁ : Tripolyphosphate concentration (%w/v)	0.1	1
X ₂ : Chitosan concentration (%w/v)	0.1	1
X ₃ : Sonication time (min)	2	10
Product quality attributes/Dependent variables		Constraints
Y ₁ : Particle size (nm)	~250 nm	
Y ₂ : Zeta Potential (mV)	~30 mV	
Y ₃ : Encapsulation efficiency (%)	Maximize	
Y ₄ : Drug release at 12 h (%)	~50%	

Table 2Model formulations of nanoparticles with the independent factors as per 3³ Face centered design.

Formulation	Tripolyphosphate concentration (%w/v)	Chitosan concentration (%w/v)	Sonication time (min)
1	0.55	0.55	6
2	1	1	2
3	1	0.1	10
4	0.55	0.55	6
5	0.1	1	10
6	0.1	0.1	2
7	0.1	0.1	10
8	0.55	0.55	6
9	1	1	10
10	1	0.1	2
11	0.55	0.55	6
12	0.1	1	2
13	0.55	0.1	6
14	0.1	0.55	6
15	1	0.55	6
16	0.55	0.55	10
17	0.55	1	6
18	0.55	0.55	6
19	0.55	0.55	6
20	0.55	0.55	2

Table 3

The response parameters/product quality attributes of model formulations of nanoparticles prepared as per 3³ Face centered design.

Formulation	Particle size (nm)	Zeta pot (mv)	Encapsulation efficiency (%)	% Release at 12 h
1	475.24 ± 12.15	27.1 ± 3.21	72.18 ± 3.26	29.44 ± 3.18
2	374.67 ± 10.86	18.2 ± 1.80	40.98 ± 4.72	19.53 ± 1.07
3	182.34 ± 15.40	20.3 ± 2.03	74.57 ± 2.48	32.76 ± 2.60
4	410.45 ± 33.67	28.5 ± 1.20	75.36 ± 3.31	34.30 ± 2.81
5	747.31 ± 59.82	26.1 ± 1.16	51.18 ± 6.20	23.58 ± 1.55
6	310.12 ± 28.21	34.3 ± 2.43	74.93 ± 2.17	40.74 ± 1.76
7	212.36 ± 21.02	38.6 ± 2.80	83.68 ± 2.08	52.52 ± 2.08
8	495.21 ± 40.20	25.9 ± 2.03	68.22 ± 1.52	29.79 ± 2.61
9	785.64 ± 68.31	20.2 ± 1.65	47.28 ± 1.97	18.66 ± 2.29
10	250.27 ± 29.53	23.6 ± 1.09	64.57 ± 1.03	29.33 ± 1.57
11	436.21 ± 36.77	27.8 ± 1.55	78.61 ± 2.95	37.42 ± 2.51
12	831.25 ± 20.94	24.0 ± 0.82	57.32 ± 1.51	19.50 ± 1.68
13	345.27 ± 37.30	30.9 ± 2.61	86.94 ± 2.03	50.46 ± 3.64
14	625.72 ± 42.88	34.1 ± 2.17	76.57 ± 1.76	38.07 ± 3.07
15	400.26 ± 39.14	16.4 ± 2.30	62.32 ± 1.33	28.37 ± 2.33
16	354.12 ± 13.56	34.6 ± 0.91	80.19 ± 1.90	34.89 ± 2.57
17	612.45 ± 60.28	27.1 ± 2.63	51.63 ± 2.83	17.01 ± 2.96
18	471.69 ± 18.20	30.6 ± 2.45	77.06 ± 2.11	48.32 ± 2.05
19	510.87 ± 31.13	31.9 ± 2.82	72.32 ± 1.48	34.60 ± 1.68
20	568.64 ± 40.32	26.7 ± 1.90	68.32 ± 1.06	28.94 ± 1.32

The values in the table represent mean ± SD of three determinations.

Table 4

Summary of ANOVA for the response parameters/product quality attributes of the model formulations of nanoparticles prepared as per 3³ Face centered design.

Response	F value	Prob > F	R ²	Adj R ²
Y ₁	25.24	<0.0001	0.75	0.72
Y ₂	18.13	<0.0001	0.68	0.64
Y ₃	34.65	<0.0001	0.93	0.89
Y ₄	17.72	<0.0001	0.68	0.64

Regression equations of the fitted models^a

$$Y_1 = 308.99 - 163.02 X_1 + 455.77 X_2$$

$$Y_2 = 38.41 - 12.98 X_1 - 7.13 X_2$$

$$Y_3 = 74.71 + 20.75 X_1 + 3.33 X_2 + 0.77 X_3 - 29.77 X_1^1 - 30.56 X_1^2$$

$$Y_4 = 51.08 - 9.95 X_1 - 23.89 X_2$$

^a Only the terms with statistical significance ($p < 0.05$) are included in the models.

Composition of the optimized formulations and comparison of the experimental values of the response parameters/product quality attributes with the predicted values.

Table 5

Formulation no.	Composition (X ₁ :X ₂ :X ₃)	Responses	Experimental value ^a	Predicted value %	Prediction error
21	0.1: 0.8: 7.25	Y ₁ (nm)	218.23 ± 20.61	224.20	-2.66
		Y ₂ (mV)	20.90 ± 1.71	27.31	-23.48
		Y ₃ (%)	71.29 ± 6.42	77.87	-8.45
		Y ₄ (%)	39.12 ± 2.80	40.72	-3.94
22	0.1:0.55: 10	Y ₁ (nm)	278.56 ± 12.90	264.66	5.25
		Y ₂ (mV)	26.71 ± 3.07	30.53	-12.53
		Y ₃ (%)	82.45 ± 2.56	84.82	-2.79
		Y ₄ (%)	52.97 ± 2.48	43.20	22.62
23	0.1:0.65:5.65	Y ₁ (nm)	245.87 ± 17.63	248.78	-1.15
		Y ₂ (mV)	29.30 ± 2.50	29.27	0.11
		Y ₃ (%)	76.66 ± 3.68	80.01	-4.19
		Y ₄ (%)	48.33 ± 1.91	42.22	14.48

^a Values represent mean ± SD (n = 3).